J Membrane Biol (2011) 243:15–23
DOI 10.1007/s00232-011-9388-0

Functional Differences in Pore Properties Between Wild-Type and Cysteine-Less Forms of the CFTR Chloride Channel

Ryan G. Holstead · Man-Song Li · Paul Linsdell

Received: 3 March 2011 / Accepted: 13 July 2011 / Published online: 28 July 2011

Abstract Studies of the structure and function of the cystic fibrosis transmembrane conductance regulator (CFTR) Cl^- channel have been advanced by the development of functional channel variants in which all 18 endogenous cysteine residues have been mutated ("cys-less" CFTR). However, cys-less CFTR has a slightly higher single-channel conductance than wild-type CFTR, raising questions as to the suitability of cys-less as a model of the wild-type CFTR pore. We used site-directed mutagenesis and patch-clamp recording to investigate the origin of this conductance difference and to determine the extent of functional differences between wild-type and cys-less CFTR channel permeation properties. Our results suggest that the conductance difference is the result of a single substitution, of C343: the point mutant C343S has a conductance similar to cys-less, whereas the reverse mutation, S343C in a cys-less background, restores wild-type conductance levels. Other cysteine substitutions (C128S, C225S, C376S, C866S) were without effect. Substitution of other residues for C343 suggested that conductance is dependent on amino acid side chain volume at this position. A range of other functional pore properties, including interactions with channel blockers ($Au[CN]_2^-$, 5-nitro-2-[3-phenylpropylamino]benzoic acid, suramin) and anion permeability, were not significantly different between wild-type and cys-less CFTR. Our results suggest that functional differences between these two CFTR constructs are of limited scale and scope and result from a small change in side chain volume at position 343. These results therefore support the use of cys-less as a model of the CFTR pore region.

Keywords Chloride channel · Cystic fibrosis transmembrane conductance regulator · Ion channel pore · Open channel block · Permeation · Selectivity · Single channel · Site-directed mutagenesis · Substituted cysteine accessibility

R. G. Holstead · M.-S. Li · P. Linsdell (✉)
Department of Physiology and Biophysics, Dalhousie University, 5850 College Street, Halifax, NS B3H 1X5, Canada
e-mail: paul.linsdell@dal.ca

Introduction

Cystic fibrosis (CF) is caused by genetic mutations that cause loss of function of the CF transmembrane conductance regulator (CFTR), an epithelial cell Cl^- channel (Gadsby et al. 2006). Understanding of normal CFTR function, as well as the molecular mechanisms of dysfunction in CF, is currently hampered by a lack of high-resolution structural information on the full-length protein. The structures of isolated, cytosolic domains of the CFTR protein that are involved in channel regulation have been solved at residue-level resolution (Lewis et al. 2004, 2005; Baker et al. 2007). In contrast, only very low-resolution imaging of the membrane-spanning parts of the protein that form the pathway for Cl^- movement has been possible (Mio et al. 2008; Zhang et al. 2009); and as a result, the structure of the transmembrane pore region is currently relatively poorly defined.

An important breakthrough in studies of the structure and function of CFTR has been the development of forms of the protein in which all 18 endogenous cysteine residues have been removed by mutagenesis, resulting in a "cys-less" CFTR (Loo and Clarke 2006). This is important to provide a background into which unique cysteine residues can be introduced and probed individually using

irreversible thiol-modifying agents. Cys-less CFTR has been used in this way to investigate the structure and function of the cytoplasmic nucleotide binding domains (NBDs) (Cui et al. 2006; Mense et al. 2006; He et al. 2008), cytoplasmic loops (He et al. 2008) and pore region (Serrano et al. 2006; Beck et al. 2008; Alexander et al. 2009; Bai et al. 2010; El Hiani and Linsdell 2010; Zhou et al. 2010). The utility of this approach is demonstrated by the fact that at least three groups have reported independently generating cys-less forms of CFTR (Cui et al. 2006; Mense et al. 2006; Wang et al. 2007).

Cys-less CFTR is difficult to traffic to the cell membrane (Loo and Clarke 2006; Wang et al. 2007); however, once resident in the membrane, it has been reported to have similar functional properties as wild-type CFTR. For example, protein kinase A (PKA)- and ATP-dependent gating at the single-channel level has been reported to be very similar (Cui et al. 2006; Mense et al. 2006). However, one notable functional difference that has been frequently (Cui et al. 2006; Mense et al. 2006; Li et al. 2009; Bai et al. 2010) but not universally (Serrano et al. 2006) reported is a small ($\sim$10–20%) increase in single-channel conductance. This functional difference has particularly strong implications for use of cys-less CFTR for studies of CFTR channel pore structure and function as it raises questions concerning how similar the permeation properties of these two channel constructs are and consequently how well a model of the wild-type channel pore is represented by the cys-less channel pore. Although cys-less has been used by several groups to investigate CFTR pore structure and function (Beck et al. 2008; Alexander et al. 2009; Bai et al. 2010; El Hiani and Linsdell 2010), the origin of this difference in conductance has not previously been investigated. In addition, functional differences between wild type and cys-less might point to previously unrecognized roles for native cysteine residues. With these points in mind, the aims of the present study were to explore both the extent and the molecular basis of functional differences between the wild-type and cys-less CFTR channel pores.

Methods

Experiments were carried out on baby hamster kidney cells transiently transfected with different forms of human CFTR. The CFTR backgrounds used were wild type (prepared as described in Gong et al. 2002) and one in which all cysteines had been removed by mutagenesis ("cys-less" CFTR; prepared as described in Mense et al. 2006; Li et al. 2009). Cys-less CFTR also included a mutation in the first NBD (V510A) to increase protein expression in the cell membrane (Li et al. 2009). The V510A mutation itself is not expected to affect single-channel conductance, which has previously been reported to be similarly increased in cys-less CFTR without (Cui et al. 2006; Mense et al. 2006) and with (Li et al. 2009; Bai et al. 2010) the V510A mutation. Transiently transfected cells were maintained at 37 °C (wild-type background) or 27 °C (cys-less background) for 1–4 days prior to patch-clamp experimentation. Mutations were introduced in these backgrounds using the QuikChange sit-directed mutagenesis system (Stratagene, La Jolla, CA) and verified by DNA sequencing.

Single-channel and macroscopic patch-clamp recordings were made using the excised, inside-out configuration of the patch-clamp technique. CFTR channels were activated after patch excision and recording of background currents by exposure to PKA catalytic subunit (5–30 nM) plus MgATP (1 mM) in the cytoplasmic solution. In some experiments using open channel blockers (see Figs. 5, 6) macroscopic currents were recorded following treatment with sodium pyrophosphate (PPi, 2 mM) to maximize channel activity and minimize changes in channel gating (Linsdell and Gong 2002; Gong and Linsdell 2003a; Fatehi et al. 2007). To ensure maximal stimulation by PPi, this substance was added after the PKA- and ATP-activated current had reached a steady amplitude. During most inside-out patch recordings, the intracellular (bath) solution contained (mM) 150 NaCl, 10 *N*-tris(hydroxymethyl)methyl-2-aminoethanesulfonate (TES) and 2 $MgCl_2$. In a small number of experiments (see Figs. 5b, 7) this same solution was used in the extracellular (pipette) solution; however, in most cases a low extracellular Cl^- concentration (4 mM) was used (NaCl replaced by Na gluconate). To estimate channel permeability to different anions (Fig. 7), NaCl in the intracellular solution was replaced by NaBr, NaI or NaSCN. All experimental solutions were adjusted to pH 7.4. All chemicals were obtained from Sigma-Aldrich (Oakville, Canada), except PKA (Promega, Madison, WI).

Current traces were filtered at 50–100 Hz using an eight-pole Bessel filter, digitized at 250 Hz–1 kHz and analyzed using pCLAMP9 software (Molecular Devices, Sunnyvale, CA). Single-channel current amplitudes were estimated from measurements of the amplitudes of individual open–closed transitions, measured using cursors set to the open and closed current levels over short periods of current record (Tabcharani et al. 1997). At least 20 individual current amplitudes were averaged for each patch at each membrane potential. Macroscopic current–voltage (*I–V*) relationships were constructed using depolarizing voltage ramp protocols (Linsdell and Hanrahan 1996, 1998). Background (leak) currents recorded before addition of PKA and ATP were subtracted digitally, leaving uncontaminated CFTR currents (Linsdell and Hanrahan 1998; Gong and Linsdell 2003a). Membrane voltages were corrected for liquid junction potentials calculated using pCLAMP9 software. As in a previous study (Zhou et al. 2010), the open channel blocking

effects of 5-nitro-2-(3-phenylpropylamino)benzoic acid (NPPB) on macroscopic current amplitude were analyzed using the simplest version of the Woodhull (1973) model of voltage-dependent block:

$$I/I_0 = K_d(V)/\{K_d(V) + [B]\} \quad (1)$$

where I is the current amplitude in the presence of blocker, I_0 the control unblocked current amplitude, [B] the blocker concentration and $K_d(V)$ the voltage-dependent apparent dissociation constant, the voltage dependence of which is given by

$$K_d(V) = K_d(0)\exp(-z\delta VF/RT) \quad (2)$$

where $z\delta$ is the effective valence of the blocking ion (actual valence z multiplied by the fraction of the transmembrane electric field apparently experienced during the blocking reaction) and F, R and T have their usual thermodynamic meanings. For block by suramin, the K_d was approximated by

$$K_d = [B]/\{[1/(I/I_0)] - 1\} \quad (3)$$

The macroscopic current reversal potential (V_{REV}) was estimated by fitting a polynomial function to the leak-subtracted I–V relationship and used to calculate the permeability of different anions (X^-) relative to that of Cl^- (P_X/P_{Cl}) according to

$$V_{REV} = (RT/F)\ln\left[\left(P_X[X]_i + P_{Cl}[Cl]_i\right)/\left(P_{Cl}[Cl]_o\right)\right] \quad (4)$$

where $[X]_i$ and $[Cl]_i$ (intracellular concentrations) are 150 and 4 mM respectively, and $[Cl]_o$ (extracellular) is 154 mM.

Experiments were carried out at room temperature, 21–24 °C. Values are presented as mean ± SEM. Tests of significance were carried out using Student's two-tailed t-test.

Results

Conductance Differences Between Wild-Type and Cys-Less CFTR

The CFTR protein contains 18 cysteine residues, the locations of which are illustrated in Fig. 1. Of these, four are found in membrane-spanning regions: C128 (TM2), C225 (TM4), C343 (TM6) and C866 (TM7) (Fig. 1). Furthermore, one cysteine is located in the second intracellular loop connecting TMs 4 and 5, and this loop has previously been suggested to contribute to the conductance properties of the channel (Xie et al. 1995). These five cysteine residues were considered of highest likelihood to influence channel conductance and were mutated individually to serines (as in cys-less CFTR).

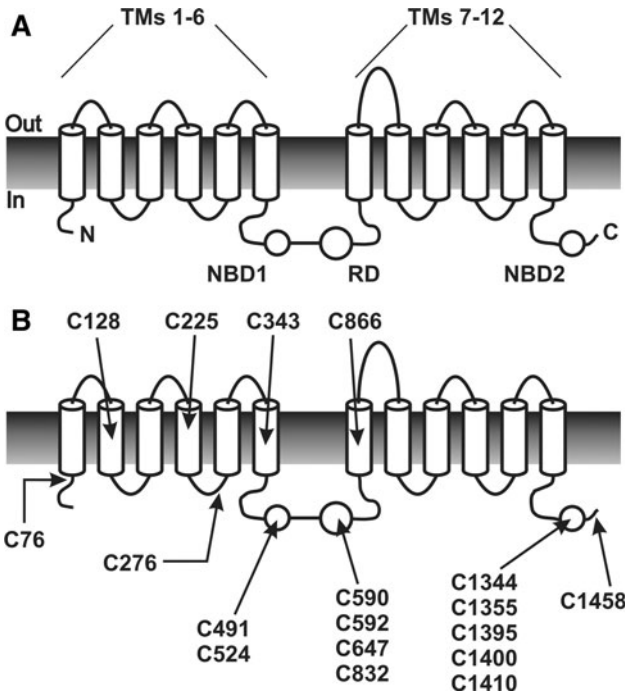

Fig. 1 Location of cysteine residues in the CFTR protein. **a** Overall topology of the CFTR protein, comprising 12 transmembrane regions (TMs 1–12), two cytoplasmic NBDs (NBD1, NBD2) and the cytoplasmic regulatory domain (RD). **b** Location of the 18 endogenous cysteines in CFTR. Those mutated in the present study were C128 (TM2), C225 (TM4), C276 (intracellular loop 3, between TM4 and TM5), C343 (TM6) and C866 (TM7). Other cysteines are found in cytoplasmic regions of the protein: N terminus (C76), NBD1 (C491, C524), RD (C590, C592, C647, C832), NBD2 (C1344, C1355, C1395, C1400, C1410) and C terminus (C1458)

Cys-less CFTR has previously been shown to have a slightly higher single-channel conductance than wild type (Mense et al. 2006; Cui et al. 2006; Li et al. 2009; see Introduction), an effect that is shown in Fig. 2. Using a low extracellular Cl^- concentration (4 mM), the unitary slope conductance was 4.75 ± 0.06 pS ($n = 11$) for wild type and 5.61 ± 0.17 pS ($n = 8$) for cys-less ($P < 0.0001$) (Fig. 1d). This increase in conductance (18.3 ± 3.5%, $n = 8$) is similar to what has been reported previously under both low (Li et al. 2009) and high (Mense et al. 2006; Cui et al. 2006) extracellular [Cl^-] conditions.

Single-channel conductance was also significantly increased in the point mutant C343S ($P < 0.0001$) (Fig. 2), albeit to a slightly lesser degree than in cys-less (14.5 ± 2.7%, $n = 8$). In fact, the conductances of cys-less and C343S were not significantly different ($P > 0.4$). In contrast, other point mutants studied (C128S, C225S, C276S, C866S) had conductances that were not significantly different from wild type but were significantly different from cys-less (Fig. 2d). This suggests that the conductance differences between wild type and cys-less result predominantly from the mutation of C343 in TM6 to a serine in this construct.

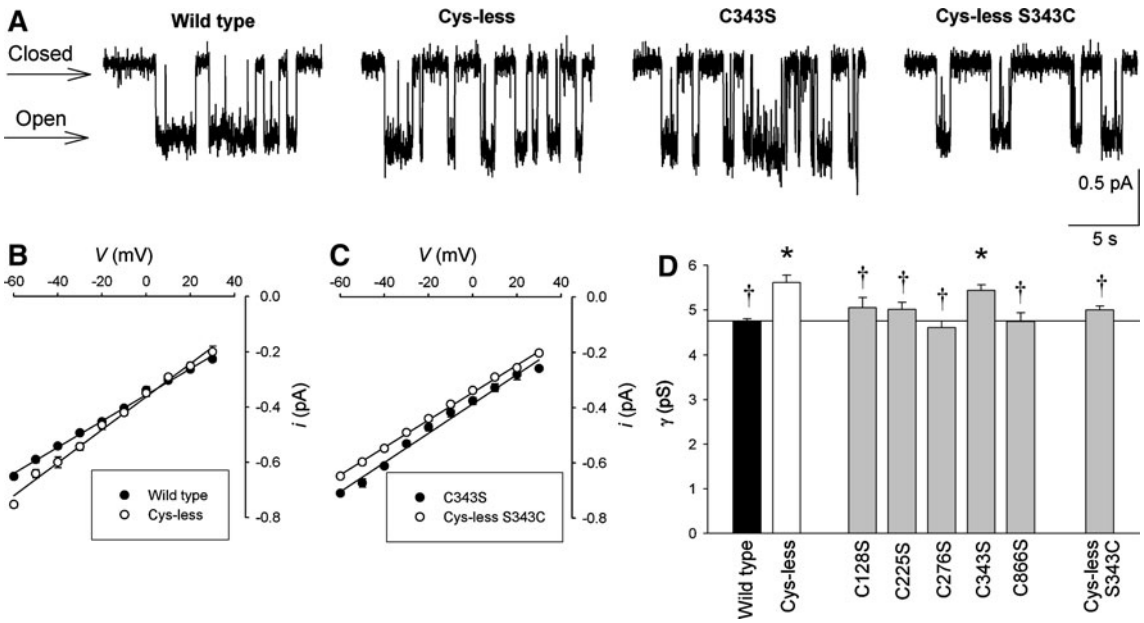

Fig. 2 Single-channel conductance of wild-type, cys-less and mutant forms of CFTR. **a** Example single-channel currents carried by the different CFTR variants named with low extracellular Cl^- concentration (4 mM), at a membrane potential of −50 mV. *Arrows to the left* indicate the closed and open channel current levels. **b**, **c** Mean single channel *I–V* relationships recorded under these conditions for wild-type (*filled circle*, **b**), cys-less (*open circle*, **b**), C343S (*filled circle*, **c**) and cys-less S343C (*open circle*, **c**). **d** Mean unitary slope conductances for different channel variants measured under these conditions. *Significant difference from wild-type, †significant difference from cys-less ($P < 0.05$ in both cases). Mean of data from 4 to 11 patches in (**b**)–(**d**)

Consistent with this hypothesis, the reverse mutation S343C in a cys-less background apparently restored the conductance phenotype of wild-type CFTR, significantly reducing cys-less single-channel conductance to a level not significantly different from that measured in wild type (Fig. 2).

Although TM6 is known to be an important determinant of CFTR pore properties (Linsdell 2006), we are unaware of any previous evidence that C343 influences unitary conductance. To investigate further the role of this amino acid, we therefore made additional substitutions at this position. As shown in Fig. 3, single-channel conductance was significantly reduced in C343L, significantly increased in C343A as well as C343S and not significantly changed in C343T and C343V. This pattern of changes suggests a size-dependent effect, with smaller amino acid side chains at this position being associated with higher single-channel conductance (Fig. 3d).

Other Functional Properties of Cys-Less CFTR

The conductance difference between wild-type and cys-less CFTR raises concerns about whether cys-less represents a good model of the CFTR pore. It is important, therefore, to understand the degree of functional similarity or difference in pore properties of these two channel variants. To this end, we compared a number of different, commonly used measures of pore function: binding of permeant and blocking ions, interactions between Cl^- and blocking ions inside the channel pore and anion selectivity.

Permeant anion binding inside the pore is relatively sensitive to the effects of mutagenesis (Mansoura et al. 1998; Ge et al. 2004), and we have previously used block of Cl^- permeation by the high-affinity permeant anion $Au(CN)_2^-$ as a functional measure of permeant anion binding within the pore (Gong et al. 2002; Ge et al. 2004; Fatehi et al. 2007). Because intracellular $Au(CN)_2^-$ affects CFTR channel gating as well as Cl^- permeation (Linsdell and Gong 2002), we isolated pore-mediated effects using single-channel recording. As shown in Fig. 4, single-channel currents carried by wild-type and cys-less CFTR were both sensitive to block by intracellular $Au(CN)_2^-$ ions. In fact, no quantitative differences in sensitivity to $Au(CN)_2^-$ were observed (Fig. 4d).

Chloride permeation in CFTR is sensitive to a wide range of impermeant open channel blocking anions acting from the cytoplasmic side of the membrane (Linsdell 2006). These inhibitors are thought to act by two different molecular mechanisms: by interacting with a relatively deep binding site in a voltage- and extracellular Cl^- concentration-dependent manner or by interacting with a relatively superficial binding site in a more voltage- and Cl^--insensitive manner (St. Aubin et al. 2007). Examples of commonly used blockers acting by these two mechanisms are NPPB (Linsdell 2005) and suramin (St. Aubin et al. 2007).

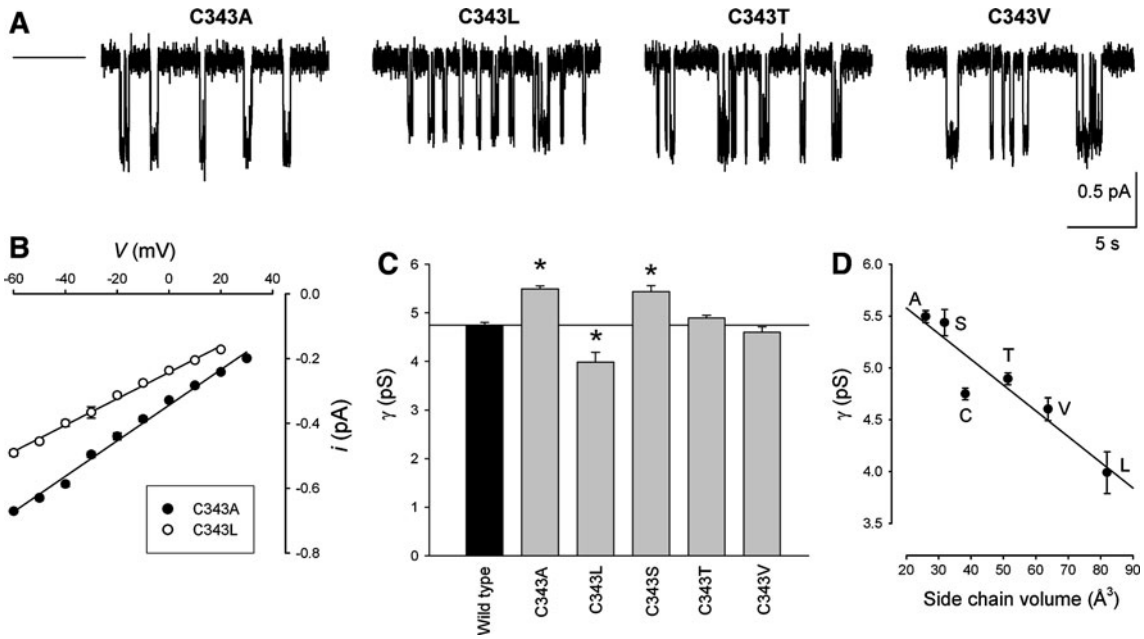

Fig. 3 Effect of mutations at C343 on single-channel conductance. **a** Example single-channel currents carried by the different CFTR variants named with low (4 mM) extracellular Cl^- concentrations, at a membrane potential of −50 mV. *Line to the left* indicates the closed channel current level. **b** Mean single channel *I–V* relationships recorded under these conditions for C343A (*filled circle*) and C343L (*open circle*). **c** Mean unitary slope conductances for different channel variants measured under these conditions. *Significant difference from wild type ($P < 0.05$). **d** Dependence of unitary conductance [as in (**c**)] on the volume of the amino acid side chain at position 343; *C* represents the wild-type cysteine residue. Side chain volumes estimated according to Richards (1974). Mean of data from 4 to 11 patches in (**b**)–(**d**)

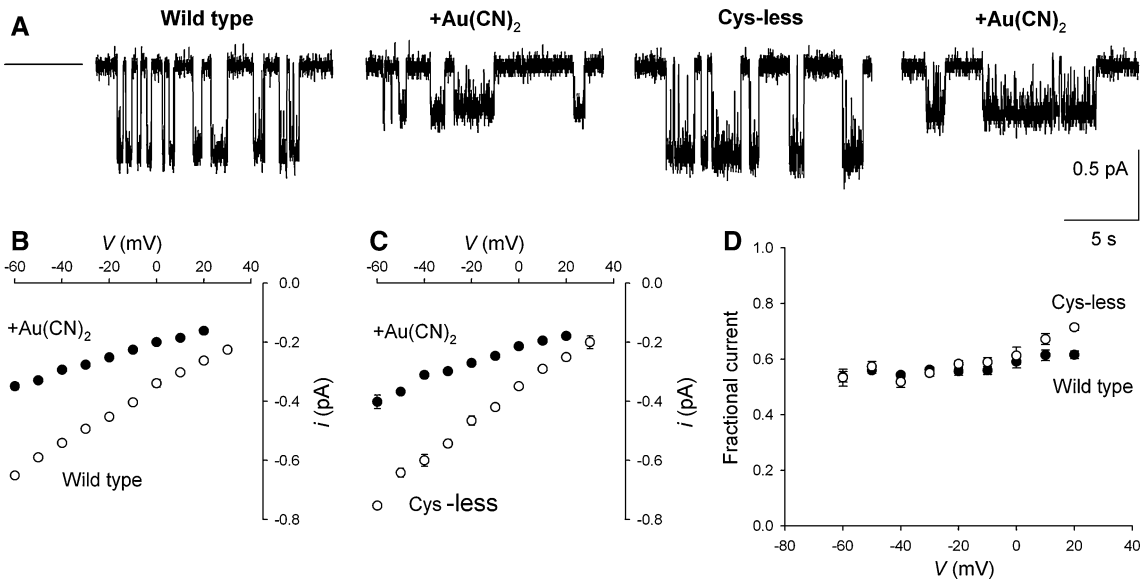

Fig. 4 Block of wild-type and cys-less CFTR by intracellular $Au(CN)_2^-$ ions. **a** Example single-channel currents carried by wild-type (*left panels*) and cys-less CFTR (*right panels*) with low extracellular Cl^- concentration (4 mM), at a membrane potential of −50 mV. *Line to the left* indicates the closed channel current level. In both cases currents were recorded in the absence or presence of 50 μM $Au(CN)_2^-$ in the intracellular solution (as indicated). **b**, **c** Mean single *I–V* relationships for wild-type (**b**) and cys-less (**c**) CFTR under these conditions, both in control (*open circle*) and in the presence of 50 μM $Au(CN)_2^-$ in the intracellular solution (*filled circle*). **d** Mean fractional unitary current remaining in the presence of this concentration of $Au(CN)_2^-$ for wild type (*filled circle*) and cys-less (*open circle*). Mean of data from three to eight patches in (**b**)–(**d**)

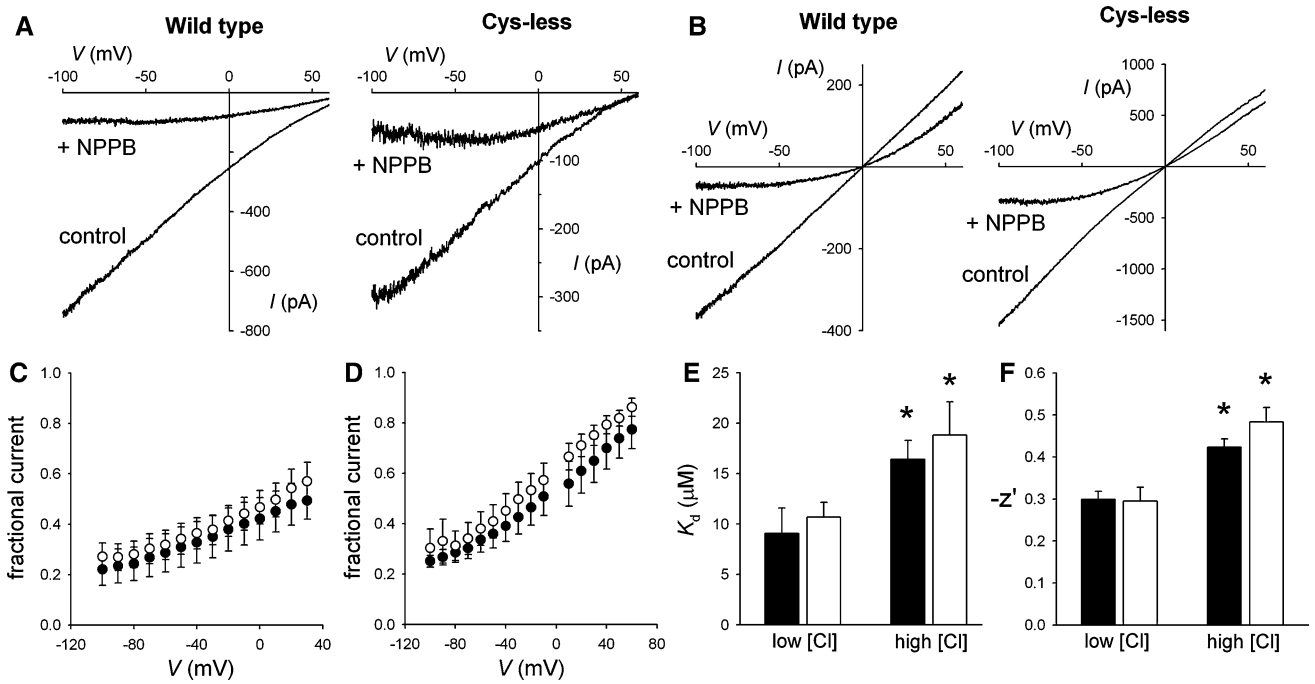

Fig. 5 Block of wild-type and cys-less CFTR by intracellular NPPB. **a**, **b** Example leak-subtracted macroscopic *I–V* relationships for wild-type and cys-less CFTR (as indicated), recorded before (control) and following addition of 10 μM NPPB to the intracellular (bath) solution. Currents were recorded using low (4 mM, **a**) or high (154 mM, **b**) extracellular Cl^- concentration. **c**, **d** Mean fractional current remaining following addition of NPPB as a function of voltage, for wild type (*filled circle*) and cys-less (*open circle*), under low (4 mM, **c**) or high (154 mM, **d**) extracellular Cl^- concentration conditions. **e** Mean $K_d(0)$ for NPPB, quantified as described in "Methods" section (Eqs. 1, 2) under low and high Cl^- concentration conditions as indicated. **f** Mean apparent valence ($-z'$) for NPPB, quantified as described in "Methods" section (Eqs. 1, 2) under low and high Cl^- concentration conditions as indicated. In both **e** and **f**, *black bars* represent wild-type and *white bars* cys-less CFTR. Mean of data from five to seven patches. *Significant difference from low [Cl^-] conditions for the same channel construct ($P < 0.05$)

Block by NPPB is shown in Fig. 5, under conditions of both low external Cl^- concentration (4 mM, Fig. 5a) and high external Cl^- concentration (154 mM, Fig. 5b). Under these conditions, NPPB causes a voltage-dependent block of CFTR current (Zhang et al. 2000; Linsdell 2005), and both the apparent affinity ($K_d[0]$, Fig. 5e) and voltage dependence (z', Fig. 5f) are dependent on extracellular Cl^- concentration. This is thought to reflect negative interactions between extracellular Cl^- ions and intracellular blocking ions inside the channel pore (Gong and Linsdell 2003b). Nevertheless, there were no apparent differences in NPPB affinity or voltage dependence between wild type and cys-less under any conditions studied (Fig. 5). This suggests that not only NPPB block but also Cl^-–blocker interactions are unaltered in cys-less CFTR.

Suramin block of wild-type and cys-less CFTR are compared in Fig. 6. As described previously (St. Aubin et al. 2007), addition of 10 μM suramin to the intracellular solution caused a potent, practically voltage-independent inhibition of wild type. The blocking effects of this concentration of suramin on cys-less CFTR appeared indistinguishable from those on wild type (Fig. 6).

Cystic fibrosis transmembrane conductance regulator shows a lyotropic anion selectivity pattern (Linsdell 2006). Anion selectivity of wild type and cys-less were compared using intracellular (bath) solutions containing different test anions (Br^-, I^-, SCN^-). As shown in Fig. 7, macroscopic current reversal potential measurements with different anions present in the bath solution showed no significant difference in the permeabilities of these anions between wild type and cys-less, with both channels showing the anion selectivity sequence $SCN^- > Br^- > Cl^- > I^-$.

Discussion

Cys-less CFTR is known to have a higher single-channel conductance than wild-type CFTR (Cui et al. 2006; Mense et al. 2006; Li et al. 2009; Bai et al. 2010), an effect that is shown in Fig. 2. In contrast, a range of experimental protocols designed to probe different aspects of pore function—binding of permeant (Fig. 4) and blocking (Figs. 5, 6) anions, interactions between a cytoplasmic blocker (NPPB) and extracellular Cl^- ions (Fig. 5) and permeability of Br^-,

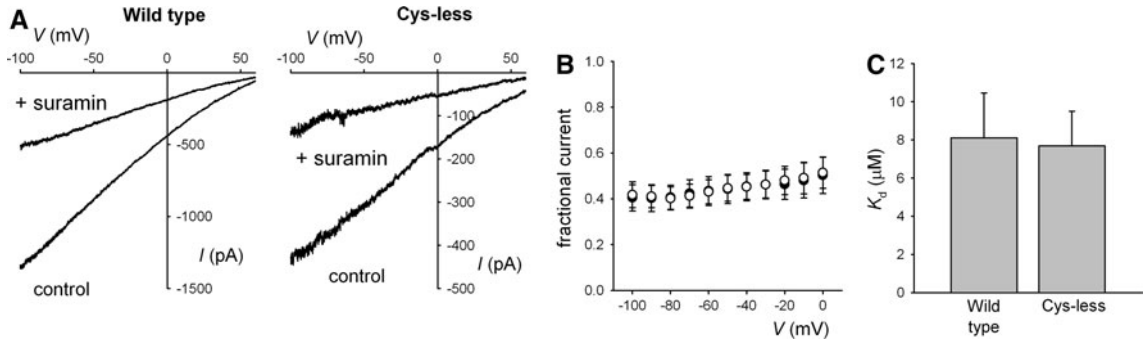

Fig. 6 Block of wild-type and cys-less CFTR by intracellular suramin. **a** Example leak-subtracted macroscopic *I–V* relationships for wild-type (*left*) and cys-less (*right*) CFTR with low extracellular Cl^- concentration (4 mM). In both cases, currents were recorded before (control) and following addition of 10 μM suramin to the intracellular (bath) solution. **b** Mean fractional current remaining following addition of suramin as a function of voltage, for wild type (*filled circle*) and cys-less (*open circle*). **c** Mean K_d for suramin, quantified at −100 mV as described in "Methods" section (Eq. 3). Mean of data from four to seven patches in (**b**)–(**c**)

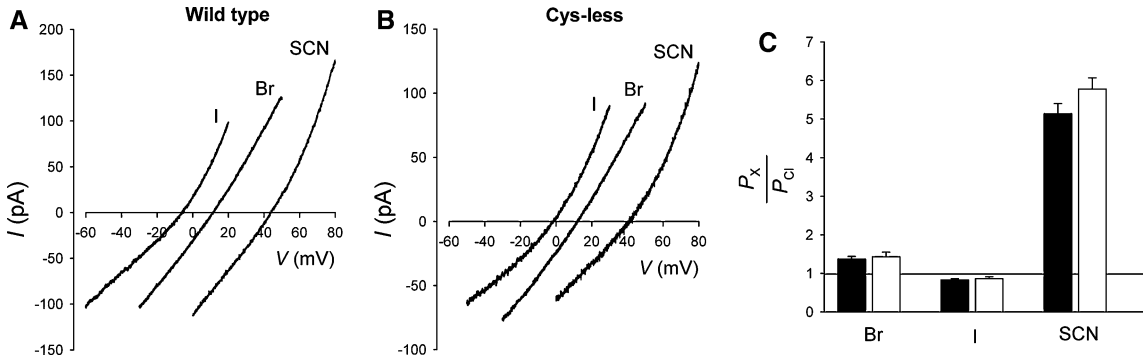

Fig. 7 Anion permeability of wild-type and cys-less CFTR. **a**, **b** Example leak-subtracted macroscopic *I–V* relationships for wild-type (**a**) and cys-less (**b**) CFTR, recorded with Cl^--containing extracellular solutions and intracellular solutions containing Br^-, I^- or SCN^- as indicated. Note that experiments with different anions were carried out on different patches and, as such, no information is contained in the relative current amplitudes with different anions. Currents reversed close to 0 mV with Cl^--containing intracellular solutions as expected (see Fig. 5b). **c** Mean P_X/P_{Cl} values calculated from reversal potential measurements under these conditions as described in "Methods" section (Eq. 4). For each anion tested, *black bars* represent wild-type and *white bars* cys-less CFTR. Mean of data from five or six patches

I^- and SCN^- ions (Fig. 7)—did not reveal any further significant differences between these two channel constructs. Previous work has identified specific mutations within the CFTR pore region that significantly alter the strength of block by cytoplasmic $Au(CN)_2^-$ (Gong et al. 2002; Ge et al. 2004), NPPB (Zhang et al. 2000; Linsdell 2005) and suramin (St. Aubin et al. 2007), as well as mutations that alter the interaction between extracellular Cl^- and cytoplasmic blocking anions (Gupta and Linsdell 2002; Zhou and Linsdell 2009), giving some information on the possible location and distribution of anion binding sites within the pore. Furthermore, mutations in several TMs have been shown to alter the permeability of different anions (Linsdell et al. 1998, 2000; Mansoura et al. 1998; McCarty and Zhang 2001; Ge et al. 2004; Fatehi and Linsdell 2009), again leading to suggestions concerning the possible mechanism of anion selectivity (Linsdell 2006). The isolated increase in unitary conductance seen in cys-less therefore suggests that the functional differences between wild-type and cys-less channel pores are highly limited in scope.

The conductance difference between wild type and cys-less appears to result predominantly from a single difference, the replacement of cysteine 343 in TM6 of wild type by a serine in cys-less. Thus, the point mutation C343S causes an increase in conductance to a near cys-less level, whereas the revertant mutation S343C in a cys-less background reduces conductance to a near wild-type level (Fig. 2). This would appear to reflect a size-dependent effect of amino acid side chain size at this position on unitary conductance, with smaller side chains favoring higher conductance (Fig. 3). Given the overwhelming evidence that the native cysteine side chain at this position in TM6 does not line the aqueous lumen of the pore (Cheung and Akabas 1996; Alexander et al. 2009; Bai et al. 2010; El Hiani and Linsdell 2010), we speculate that

mutation of this cysteine leads to a subtle change in packing and/or orientation of the TMs, resulting in a minor change in unitary conductance. To put this effect in context, mutation of many other TM6 residues, including R334, K335, F337, T338 and S341, has previously been shown to have a greater effect on conductance (Sheppard et al. 1993; McDonough et al. 1994; Linsdell et al. 1998; Linsdell 2001; Smith et al. 2001; Ge et al. 2004; Gong and Linsdell 2004; Bai et al. 2010).

Overall the functional differences between wild-type and cys-less CFTR channel pores appear to be of limited scale and scope and to reflect predominantly a minor change in TM arrangement due to a small change in volume of a non-pore-lining side chain. Since C343T (unlike C343S) was not associated with a significant change in single-channel conductance (Fig. 3), a cys-less construct in which C343 is replaced by threonine, rather than serine, might be considered to retain wild-type channel properties more faithfully. However, since most other permeation properties of cys-less were found to be indistinguishable between wild-type and cys-less (containing the C343S mutation), it seems likely that in most respects it is functionally inconsequential if this site is a cysteine, serine or threonine. Overall, cys-less would appear to be a good functional and, likely, structural model of the wild-type CFTR pore.

Acknowledgments We thank Drs. Yassine El Hiani, Feng Qian and Wuyang Wang for assistance. This work was supported by the Canadian Institutes of Health Research. R. G. H. was supported by the Karen Lackey Summer Studentship Award from Cystic Fibrosis Canada.

References

Alexander C, Ivetac A, Liu X, Norimatsu Y, Serrano JR, Landstrom A, Sansom M, Dawson DC (2009) Cystic fibrosis transmembrane conductance regulator: using differential reactivity toward channel-permeant and channel-impermeant thiol-reactive probes to test a molecular model for the pore. Biochemistry 48:10078–10088

Bai Y, Li M, Hwang T-C (2010) Dual roles of the sixth transmembrane segment of the CFTR chloride channel in gating and permeation. J Gen Physiol 136:293–309

Baker JM, Hudson RP, Kanelis V, Choy WY, Thibodeau PH, Thomas PJ, Forman-Kay JD (2007) CFTR regulatory region interacts with NBD1 predominantly via multiple transient helices. Nat Struct Mol Biol 14:738–745

Beck EJ, Yang Y, Yaemsiri S, Raghuram V (2008) Conformational changes in a pore-lining helix coupled to CFTR channel gating. J Biol Chem 283:4957–4966

Cheung M, Akabas MH (1996) Identification of cystic fibrosis transmembrane conductance regulator channel-lining residues in and flanking the M6 membrane-spanning segment. Biophys J 70:2688–2695

Cui L, Aleksandrov L, Hou Y-X, Gentzsch M, Chen J-H, Riordan JR, Aleksandrov AA (2006) The role of cystic fibrosis transmembrane conductance regulator phenylalanine 508 side chain in ion channel gating. J Physiol 572:347–358

El Hiani Y, Linsdell P (2010) Changes in accessibility of cytoplasmic substances to the pore associated with activation of cystic fibrosis transmembrane conductance regulator chloride channel. J Biol Chem 285:32126–32140

Fatehi M, Linsdell P (2009) Novel residues lining the CFTR chloride channel pore identified by functional modification of introduced cysteines. J Membr Biol 228:151–164

Fatehi M, St. Aubin CN, Linsdell P (2007) On the origin of asymmetric interactions between permeant anions and the CFTR chloride channel pore. Biophys J 92:1241–1253

Gadsby DC, Vergani P, Csanády L (2006) The ABC protein turned chloride channel whose failure causes cystic fibrosis. Nature 440:477–483

Ge N, Muise CN, Gong X, Linsdell P (2004) Direct comparison of the functional roles played by different transmembrane regions in the cystic fibrosis transmembrane conductance regulator chloride channel pore. J Biol Chem 279:55283–55289

Gong X, Linsdell P (2003a) Mutation-induced blocker permeability and multi-ion block of the CFTR chloride channel pore. J Gen Physiol 122:673–687

Gong X, Linsdell P (2003b) Coupled movement of permeant and blocking ions in the CFTR chloride channel pore. J Physiol 549:375–385

Gong X, Linsdell P (2004) Maximization of the rate of chloride conduction in the CFTR channel pore by ion–ion interactions. Arch Biochem Biophys 426:78–82

Gong X, Burbridge SM, Cowley EA, Linsdell P (2002) Molecular determinants of Au(CN)2-binding and permeability within the cystic fibrosis transmembrane conductance regulator Cl^- channel pore. J Physiol 540:39–47

Gupta J, Linsdell P (2002) Point mutations in the pore region directly or indirectly affect glibenclamide block of the CFTR chloride channel. Pflugers Arch 443:739–747

He L, Aleksandrov AA, Serohijos AWR, Hegedüs T, Aleksandrov LA, Cui L, Dokholyan NV, Riordan JR (2008) Multiple membrane-cytoplasmic domain contacts in the cystic fibrosis transmembrane conductance regulator (CFTR) mediate regulation of channel gating. J Biol Chem 283:26383–26390

Lewis HA, Buchanan SG, Burley SK, Conners K, Dickey M, Dorwart M, Fowler R, Gao X, Guggino WB, Hendrickson WA, Hunt JF, Kearins MC, Lorimer D, Maloney PC, Post KW, Rajashankar KR, Rutter ME, Sauder JM, Shriver S, Thibodeau PH, Thomas PJ, Zhang M, Zhao X, Emtage S (2004) Structure of nucleotide-binding domain 1 of the cystic fibrosis transmembrane conductance regulator. EMBO J 23:282–293

Lewis HA, Zhao X, Wang C, Sauder JM, Rooney I, Noland BW, Lorimer D, Kearnis MC, Conners K, Condon B, Maloney PC, Guggino WB, Hunt JF, Emtage S (2005) Impact of the ΔF508 mutation in first nucleotide-binding domain of human cystic fibrosis transmembrane conductance regulator on domain folding and structure. J Biol Chem 280:1346–1353

Li M-S, Demsey AFA, Qi J, Linsdell P (2009) Cysteine-independent inhibition of the CFTR chloride channel by the cysteine-reactive reagent sodium (2-sulphonatoethyl) methanethiosulphonate (MTSES). Br J Pharmacol 157:1065–1071

Linsdell P (2001) Relationship between anion binding and anion permeability revealed by mutagenesis within the cystic fibrosis transmembrane conductance regulator chloride channel pore. J Physiol 531:51–66

Linsdell P (2005) Location of a common inhibitor binding site in the cytoplasmic vestibule of the cystic fibrosis transmembrane conductance regulator chloride channel pore. J Biol Chem 280:8945–8950

Linsdell P (2006) Mechanism of chloride permeation in the cystic fibrosis transmembrane conductance regulator chloride channel. Exp Physiol 91:123–129

Linsdell P, Gong X (2002) Multiple inhibitory effects of $Au(CN)_2^-$ ions on cystic fibrosis transmembrane conductance regulator Cl^- channel currents. J Physiol 540:29–38

Linsdell P, Hanrahan JW (1996) Disulphonic stilbene block of cystic fibrosis transmembrane conductance regulator Cl^- channels expressed in a mammalian cell line and its regulation by a critical pore residue. J Physiol 496:687–693

Linsdell P, Hanrahan JW (1998) Adenosine triphosphate-dependent asymmetry of anion permeation in the cystic fibrosis transmembrane conductance regulator chloride channel. J Gen Physiol 111:601–614

Linsdell P, Zheng S-X, Hanrahan JW (1998) Non-pore lining amino acid side chains influence anion selectivity of the human CFTR Cl^- channel expressed in mammalian cell lines. J Physiol 512:1–16

Linsdell P, Evagelidis A, Hanrahan JW (2000) Molecular determinants of anion selectivity in the cystic fibrosis transmembrane conductance regulator chloride channel pore. Biophys J 78:2973–2982

Loo TW, Clarke DM (2006) Using a cysteine-less mutant to provide insight into the structure and mechanism of CFTR. J Physiol 572:312

Mansoura MK, Smith SS, Choi AD, Richards NW, Strong TV, Drumm ML, Collins FS, Dawson DC (1998) Cystic fibrosis transmembrane conductance regulator (CFTR) anion binding as a probe of the pore. Biophys J 74:1320–1332

McCarty NA, Zhang Z-R (2001) Identification of a region of strong discrimination in the pore of CFTR. Am J Physiol Lung Cell Mol Physiol 281:L852–L867

McDonough S, Davidson N, Lester HA, McCarty NA (1994) Novel pore-lining residues in CFTR that govern permeation and open-channel block. Neuron 13:623–634

Mense M, Vergani P, White DM, Altberg G, Nairn AC, Gadsby DC (2006) In vivo phosphorylation of CFTR promotes formation of a nucleotide-binding domain heterodimer. EMBO J 25:4728–4739

Mio K, Ogura T, Mio M, Shimizu H, Hwang T-C, Sato C, Sohma Y (2008) Three-dimensional reconstruction of human cystic fibrosis transmembrane conductance regulator chloride channel revealed an ellipsoidal structure with orifices beneath the putative transmembrane domain. J Biol Chem 283:30300–30310

Richards FM (1974) The interpretation of protein structures: total volume, group volume distributions and packing density. J Mol Biol 82:1–14

Serrano JR, Liu X, Borg ER, Alexander CS, Shaw CF, Dawson DC (2006) CFTR: ligand exchange between a permeant anion ($[Au(CN)_2]^-$) and an engineered cysteine (T338C) blocks the pore. Biophys J 91:1737–1748

Sheppard DN, Rich DP, Ostedgaard LS, Gregory RJ, Smith AE, Welsh MJ (1993) Mutations in CFTR associated with mild-disease-form Cl^- channels with altered pore properties. Nature 362:160–164

Smith SS, Liu X, Zhang Z-R, Sun F, Kriewall TE, McCarty NA, Dawson DC (2001) CFTR: covalent and noncovalent modification suggests a role for fixed charges in anion conduction. J Gen Physiol 118:407–431

St. Aubin CN, Zhou J-J, Linsdell P (2007) Identification of a second blocker binding site at the cytoplasmic mouth of the cystic fibrosis transmembrane conductance regulator chloride channel pore. Mol Pharmacol 71:1360–1368

Tabcharani JA, Linsdell P, Hanrahan JW (1997) Halide permeation in wild-type and mutant cystic fibrosis transmembrane conductance regulator chloride channels. J Gen Physiol 110:341–354

Wang Y, Loo TW, Bartlett MC, Clarke DM (2007) Correctors promote maturation of cystic fibrosis transmembrane conductance regulator (CFTR)-processing mutants by binding to the protein. J Biol Chem 282:33247–33251

Woodhull AM (1973) Ionic blockage of sodium channels in nerve. J Gen Physiol 61:687–708

Xie J, Drumm ML, Ma J, Davis PB (1995) Intracellular loop between transmembrane segments IV and V of cystic fibrosis transmembrane conductance regulator is involved in regulation of chloride channel conductance. J Biol Chem 270:28084–28091

Zhang Z-R, Zeltwanger S, McCarty NA (2000) Direct comparison of NPPB and DPC as probes of CFTR expressed in *Xenopus* oocytes. J Membr Biol 175:35–52

Zhang L, Aleksandrov LA, Zhao Z, Birtley JR, Riordan JR, Ford RC (2009) Architecture of the cystic fibrosis transmembrane conductance regulator protein and structural changes associated with phosphorylation and nucleotide binding. J Struct Biol 167:242–251

Zhou J-J, Linsdell P (2009) Evidence that extracellular anions interact with a site outside the CFTR chloride channel pore to modify channel properties. Can J Physiol Pharmacol 87:387–395

Zhou J-J, Li M-S, Qi J, Linsdell P (2010) Regulation of conductance by the number of fixed positive charges in the intracellular vestibule of the CFTR chloride channel pore. J Gen Physiol 135:229–245